Fusion and fission pathways of vesicles from amphiphilic triblock copolymers: a dissipative particle dynamics simulation study

Xuejin Li,[ab] Yuan Liu,[ab] Lei Wang,[ab] Mingge Deng[ab] and Haojun Liang*[ab]

Received 9th October 2008, Accepted 12th February 2009
First published as an Advance Article on the web 10th March 2009
DOI: 10.1039/b817773b

Dissipative particle dynamics (DPD) simulations are employed to study the fusion and fission dynamics of polymeric vesicles formed from amphiphilic triblock copolymers. The amphiphilic molecule is built from two hydrophilic blocks and a hydrophobic middle block. Two different pathways for both fusion and fission processes of two-component vesicles with polymer-based symmetric membranes have been found in the simulations. For each of the pathways, the conditions required to obtain complete fusion and fission have been investigated. Moreover, the fission process of single-component vesicles with polymer-based asymmetric membranes has also been studied in the simulations. Interestingly, the daughter vesicles have the same composition as the parent vesicle and only one fission pathway has been observed. Furthermore, the fusion and fission pathways have been compared and distinct vesicle recycling pathways have been suggested according to the results from the simulations. These findings may be helpful in explaining the fusion and fission dynamics of vesicles and understanding the general principle of membranes.

1. Introduction

The fusion and fission of vesicles in membrane transformations, in which two membranes merge and split, underlies the fundamental biological processes in normal and pathological conditions.[1,2] Study of shape transformations and topological changes such as the fusion and fission of vesicles, has important physical and biological significance. However, the kinetic and mechanistic details of these processes remain incompletely understood. Moreover, they are extremely challenging to observe directly in experiments due to the complexity of membranes and the high energy-cost of these processes. This experimental challenge makes vesicle fusion and fission an ideal target for theoretical and modeling studies. For the fusion process, theoretical studies such as the original stalk model[3–5] and the modified stalk model[6] for the fusion pore opening process, and modeling systems such as the continuum model[7] and particle-based models,[8–16] have suggested that this process is initiated by the formation of a stalk intermediate. After that, a branched pathway[8,13,16] for fusion pore opening has been suggested in which the stalk can either form a fusion pore directly or extend to a hemifusion intermediate that slowly develops a fusion pore to a complete fusion. The stable hemifused structures have been observed experimentally.[17–20] Much attention has been paid to the fission process of vesicles as well as to the fusion process. Budding and fission have been observed in both single-component and multicomponent vesicles. For single-component vesicles, complete fission can be induced by the spontaneous curvature of the membranes and the area difference between the inner and outer monolayers of the membranes.[21,22] For two-component vesicles, complete fission can also be induced by the local asymmetry in the composition between two halves of the membrane.[21,23,24] Computer simulations using solvent free method[25] and particle-based models[26–32] have suggested that the fission process to be initiated by the formation of a vesicle with multi-domains. After that, complete fission can be obtained either by cleavage along the domain boundary or through a deformation of the vesicle and a hemifission intermediate.

Presently, vesicles can be prepared from compounds such as surfactants, phospholipids and block copolymers. Their common feature is the presence of hydrophilic heads and hydrophobic tails in the molecules. Polymeric vesicles with excellent stability have attracted considerable attention in recent years for both theoretical and experimental studies.[17,33,34] However, compared with the large amount of articles on the membrane fusion and fission of lipid vesicles, papers on polymeric vesicle fusion and fission have seldom been reported. The fusion dynamics of polymeric vesicles have been first investigated by Eisenberg and his colleagues,[17] and recent experiments have shown real-time membrane fusion and fission processes of giant polymeric vesicles.[19,35] In theoretical and modeling research, these processes have been only studied by Yamamoto *et al.*[26] and Noguchi *et al.*[8,27] However, to the best of our knowledge, no studies concerning the fusion and fission dynamics of vesicles with polymer-based asymmetric membranes using particle-based models have been reported. In this article, we study the fusion and fission dynamics of polymeric vesicles using a dissipative particle dynamics (DPD) simulation.

In order to simulate polymer-based asymmetric membranes as well as vesicles in solvent, we consider the amphiphilic triblock copolymer. We show that even using relatively simple

---

[a] *CAS Key Laboratory of Soft Matter Chemistry, Department of Polymer Science and Engineering, University of Science and Technology of China, Hefei, Anhui 230026, PR China. E-mail: hjliang@ustc.edu.cn*
[b] *Hefei National Laboratory for Physical Sciences at Microscale, University of Science and Technology of China, Hefei, Anhui 230026, PR China*

models for amphiphilic triblock copolymers, many characteristics of amphiphiles in a dilute solution can be elucidated, such as their self-assembly into bilayer membranes and spontaneous formation of vesicles, as well as the distinct fusion and fission dynamics of such vesicles.

2. Simulation details

2.1 DPD formulation

Dissipative particle dynamics is a mesoscopic simulation method, introduced in 1992 by Hoogerbrugge and Koelman.[36] In DPD simulation, a particle represents the center of mass of a cluster of atoms and the mass, length, and timescales are all unity. Particles i and j interact with each other *via* a pairwise additive force, consisting of three contributions: (i) a conservative force, F_{ij}^{C}; (ii) a dissipative force, F_{ij}^{D}; and (iii) a random force, F_{ij}^{R}. Hence, the total force on particle i is given by

$$F_i = \sum_{i \neq j} F_{ij}^{\mathrm{C}} + F_{ij}^{\mathrm{D}} + F_{ij}^{\mathrm{R}}, \tag{1}$$

where the sum acts over all particles within the cutoff radius, r_{c}. Specifically, in our simulations,

$$F_i = \sum_{i \neq j} a_{ij}\omega(r_{ij})\hat{r}_{ij} - \gamma\omega^2(r_{ij})(\hat{r}_{ij} \cdot \nu_{ij})\hat{r}_{ij} + \sigma\omega(r_{ij})\zeta_{ij}\Delta t^{-1/2}\hat{r}_{ij}, \tag{2}$$

where a_{ij} is a maximum repulsion between particles i and j, r_{ij} is the distance between them, with the corresponding unit vector $\hat{r}_{ij}$, ν_{ij} is the difference between the two velocities, ζ_{ij} is a random number with zero mean and unit variance, and γ and σ are parameters coupled by $\sigma^2 = 2\gamma k_{\mathrm{B}}T$. The weighting function $\omega(r_{ij})$ is given by

$$\omega(r_{ij}) = \begin{cases} 1 - r_{ij}/r_{\mathrm{s}} & r_{ij} < r_{\mathrm{c}} \\ 0 & r_{ij} \geq r_{\mathrm{c}} \end{cases}. \tag{3}$$

The standard values $\sigma = 3.0$ and $\gamma = 4.5$ are used in our study. By joining consecutive particles with a spring force, one can construct coarse-grained models of polymers.[37,38] The harmonic spring force with a spring constant $k_{\mathrm{s}} = 4.0$ and an equilibrium bond length $r_{\mathrm{s}} = 0.86$ in our simulations has the form:

$$F_{ij}^{\mathrm{S}} = k_{\mathrm{s}}(1 - r_{ij}/r_s)\hat{r}_{ij}. \tag{4}$$

The simulations are performed using a modified version of the DPD code named MYDPD.[39] The time integration of motion equations is done using a modified velocity–Verlet algorithm with $\lambda = 0.65$ and time step $\Delta t = 0.04\tau$.

2.2 DPD models

Within the mesoscopic approach, an amphiphilic molecule is represented by a coarse-grained model. In order to simulate polymer-based asymmetric membranes as well as vesicles in solvent, we consider the amphiphilic linear triblock copolymers. For the sake of simplicity, each amphiphilic molecule is built by one hydrophilic particle (denoted by A/C) on each side and eight hydrophobic particles (denoted by B) in the middle. Solvent particles (denoted by S) are included explicitly in the simulations; however, for clarity, they are not shown in the figures. For a comparative study, both the two-component vesicles with polymer-based symmetric membranes formed from amphiphilic ABA molecules and single-component vesicles with polymer-based asymmetric membranes formed from amphiphilic ABC molecules are simulated. A spherical vesicle with a symmetric membrane that is prepared first from 9600 constituent particles of ABA amphiphilc molecules in a simulation box of 40 × 40 × 40 with a particle number density of 3. The setup for the fusion process of two-component polymeric vesicles is made by duplicating the simulation box with the vesicle inside. Two duplicate vesicles, which are reassigned by two different types of amphiphilic molecules (denoted by $\mathrm{A_\alpha B_\alpha A_\alpha}$ and $\mathrm{A_\beta B_\beta A_\beta}$), are translated and placed close to each other in a larger simulation box, such that the vesicles start at a relatively small distance from each other. For the fission process of two-component polymeric vesicles, the initial configuration is derived from the final configuration of vesicle fusion. The repulsive interaction parameters between any two particles are given by

$$a_{ij} = \left(\begin{array}{llllll} & \mathrm{A_\alpha} & \mathrm{B_\alpha} & \mathrm{A_\beta} & \mathrm{B_\beta} & \mathrm{S} \\ \mathrm{A_\alpha} & 25 & 200 & a_{\mathrm{A_\alpha A_\beta}} & 200 & 25 \\ \mathrm{B_\alpha} & 200 & 25 & 200 & a_{\mathrm{B_\alpha B_\beta}} & 200 \\ \mathrm{A_\beta} & a_{\mathrm{A_\alpha A_\beta}} & 200 & 25 & 200 & 25 \\ \mathrm{B_\beta} & 200 & a_{\mathrm{B_\alpha B_\beta}} & 200 & 25 & 200 \\ \mathrm{S} & 25 & 200 & 25 & 200 & 25 \end{array}\right) \tag{5}$$

where the repulsive parameters of $a_{\mathrm{A_\alpha A_\beta}}$ and $a_{\mathrm{B_\alpha B_\beta}}$ are varied in the simulations. Specifically values of these parameters are given in Table 1. Within these parameters, different fusion and fission pathways of two-component polymeric vesicles are observed.

The fission dynamics of single-component vesicles with polymer-based asymmetric membrane are also studied in the work. The initial configuration for these fission events starts directly from a spherical vesicle with asymmetric membrane that is formed from 9600 constituent particles of amphiphilic ABC molecules. To our knowledge, it is the first time to explore the fission dynamics of single-component vesicles with asymmetric membranes using particle-based models.

2.3 Physical length- and time-scales

In DPD approach, it is convenient to use reduced units.[37] The unit of length is defined by the cutoff radius r_{c}; the unit of the mass is defined by the masses of particles; and the unit of energy is define by $k_{\mathrm{B}}T$. Here, we will give an estimate of the physical length- and time-scales in our DPD simulations. Within the DPD approach, some molecules of the system are coarse-grained by a set of particles with a necessary assumption that each particle has the same volume based on the CG mapping on that of water, that is, the amount of matter contained in each particle is constant for all species. The value of repulsion parameter for water-like particles is chosen such that the simulated compressibility of water particles at room temperature corresponds to the experimental

Table 1 Overview of vesicle fusion and fission simulations performed with various parameters. The symbols in the TABLE denote: N_P represents the total number of particles in simulation box; N_P_ABA and N_P_ABC represent the total number of symmetric and asymmetric amphiphilic triblock copolymers, respectively. FUS-I and FUS-II represent two different fusion pathways, whereas FIS-I and FIS-II represent two different fission pathways, respectively

	Particle number			Repulsive interaction parameters							
Label	N_P	N_P_ABA	$\varphi_{A\alpha B\alpha A\alpha}$	$a_{AiAj(i,j=\alpha,\beta)}$			$a_{BiBj(i,j=\alpha,\beta)}$			k_BT	Result
FUS-SIM-I	384 000	19 200	0.50	25.0			25.0			1.00	FUS-I
FUS-SIM-II	384 000	19 200	0.50	25.0			40.0			1.00	FUS-II
				$a_{A\alpha A\alpha}$	$a_{A\beta A\beta}$	$a_{A\alpha A\beta}$	$a_{B\alpha B\alpha}$	$a_{B\beta B\beta}$	$a_{B\alpha B\beta}$		
FIS-SIM-I	384 000	19 200	0.50	25.0	25.0	100.0	25.0	25.0	100.0	1.00	FIS-I
FIS-SIM-II	384 000	19 200	0.50	25.0	25.0	100.0	25.0	25.0	100.0	1.10	FIS-II
		N_P_ABC		a_{AA}	a_{CC}	a_{AC}		a_{BB}			
FIS-SIM-III	192 000	9600		30.0	20.0	100.0		25.0		1.10	FIS-I
FIS-SIM-IV	192 000	9600		35.0	15.0	100.0		25.0		1.00	FIS-I

value. Generally, it has been previously proposed that the following equation should hold in a DPD system:

$$\frac{1}{k_BT}\left(\frac{\partial P}{\partial \rho}\right)_{\text{sim.}} = \frac{N_m}{k_BT}\left(\frac{\partial P}{\partial n}\right)_{\text{exp.}}, \tag{6}$$

where ρ and n are, respectively, the particle density of the DPD system and the density of water-like molecules in the water-like liquid. The repulsive parameter between two water-like molecules has been chosen at $a_{ii} = 25.0$, the correct compressibility of water-like particle at room temperature is matched when the value of the number of water-like molecules per DPD particle is given by $N_m = 1$. Since the simulated particle number density is $\rho r_c = 3$ and a water molecule has the volume of approximately 30 Å^3, a cube that contains three DPD particles therefore corresponds to a volume of approximately 90 Å^3; thus, we find the physical length scale of interaction radius by:

$$r_c = \sqrt[3]{90} = 0.48 \text{ nm}. \tag{7}$$

Thus, the original vesicle with a radius of approximately $10.28r_c$ has a diameter around 9.86 nm.

The effective time scale of the simulation can be found by matching the lateral diffusion constants of lipid bilayer in the simulation to that of experimentally measured values by Lipowsky and his colleagues.[40,41] To obtain the simulated diffusion constant, a DPD system consisting of an amphiphilic bilayer is simulated in a periodic box, where the bilayer is oriented perpendicular to the x-axis, and the lateral diffusion constant is determined by

$$D_L(t)_{\text{DPD}} = \frac{\sum_i [\Delta r_L(t) - \Delta r_L(0)]^2}{6Nt}, \tag{8}$$

where $\Delta r_L(t)$ is the lateral component of particle displacements relative to the center of mass of the amphiphilic bilayer. For details of this calculation that we used are available elsewhere.[40] For large time t, the lateral diffusion constant attains constant value as shown in Fig. 1. The simulated value of lateral diffusion constant of the amphiphilic molecule is given by 0.019. The quality interfacial tension is then obtained,

$$D_L(t)_{\text{calc.}} = \frac{r_c^2}{\tau} D_L(t)_{\text{DPD}}, \tag{9}$$

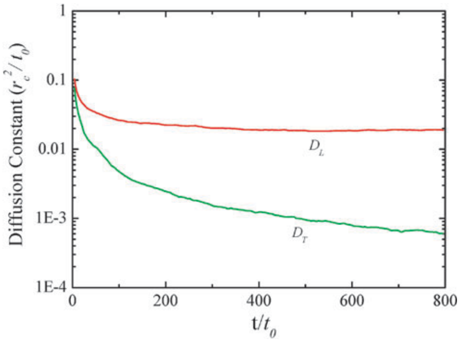

Fig. 1 The time evolution of the effective diffusion constants for amphiphilic molecules. The red and green lines represent the effective diffusion constants for lateral and transverse diffusion of amphiphilies, respectively.

which can be directly compared with the experimentally obtained diffusion constant. Compared with a typical experimental value 5 μm^2 s^{-1}, we obtain τ close to 0.87 ns. In our simulations, a constant time step of $\Delta t = 0.04\tau$ is used, thus, the time step of $\Delta t = 0.035$ ns is taken in the simulations.

3. Results and discussion

In this section, we present results from simulations of the two-component vesicles with polymer-based symmetric membranes and single-component vesicles with polymer-based asymmetric membranes. We have performed systematic simulations under various conditions by changing the following parameters:

(i) the strength of repulsive interactions for two-component vesicles. In the fusion process of polymeric vesicles, only the parameter $a_{B\alpha B\beta}$ is changed in the simulations. Whereas, in order to consider the segregation between two types of amphiphilic molecules, both the repulsive parameters of $a_{A\alpha A\beta}$ and $a_{B\alpha B\beta}$ are varied in the fission process;

(ii) the reduced volume of vesicle in the fission process. The reduced volume is the ratio of the actual volume of the vesicle to the volume of a spherical vesicle with the same area as the vesicle.[21,22] This parameter is induced by changing the systematic temperature (k_BT) or removing a certain number of solvent particles from the interior of vesicle and place into the outer region;

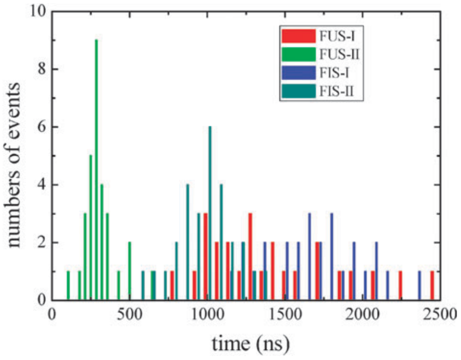

Fig. 2 Cumulative histograms of observed fusion and fission times for two-component polymeric vesicles. The different colors used in the histogram correspond to different fusion and fission processes within different parameters.

(iii) the spontaneous curvature of asymmetric membrane. For single-component vesicles consisting of amphiphilic triblock copolymers, the spontaneous curvature can be controlled by changing the repulsive parameters between two different hydrophilic particles.

An overview of the performed simulations with changing these parameters is summarized in Table 1. Fusion and fission statistics are collected by running 30 independent simulations under different conditions by changing these parameters. For vesicle fusion processes, we obtain the fusion pathway FUS-I in 25 times among 30 fusion attempts, and the fusion pathway FUS-II is observed in all 30 fusion attempts. For vesicle fission processes, we observed the fission pathway FIS-I in 26 of 30 examined fission events, and the fission pathway FIS-II is observed in 28 times among 30 examined fission events. The cumulative histogram for the observed fusion times of two-component polymeric vesicles is shown in Fig. 2. In the following sections, several fusion and fission pathways of polymeric vesicles are observed and different conditions required to obtain complete fusion and fission for each of the pathways are investigated.

3.1 Vesicle fusion

As we stated earlier, the setup for the fusion process of two-component polymeric vesicles is made by duplicating the simulation box with the vesicle inside, both duplicated vesicles are translated and placed close to each other in a larger simulation box.

In a typical fusion pathway (FUS-I), this process starts from two vesicles come into close contact and form a stalk (Fig. 3a). Expansion of the stalk leads first, to touching of inner monolayer inside the stalk, (Fig. 3b) and second, to developing of an extended hemifusion intermediate that a disk-like bilayer consisting of both inner monolayers (Fig. 3c). A small fusion pore is then developed in this bilayer (Fig. 3d), whose expansion completes fusion with the formation of a larger vesicle (Fig. 3e). Finally, diffusion of particles from two different types of amphiphilic molecules results in a vesicle with an approximately homogeneous distribution (Fig. 3f). This fusion pathway of two-component vesicles agrees well with the original stalk model.[3–5] In a previous study, two different fusion pathways of vesicles have been found by Noguchi *et al.*[8] using a Brownian dynamic simulation; however, the pore-opening pathway in the original stalk model was not seen in their simulations and molecules with long flexible hydrophobic tails were proposed to observe this fusion pathway. In our simulations, the amphiphilic molecule is built from two hydrophilic particles and eight hydrophobic particles, and a longer flexible hydrophobic block can be modeled. The observation of this fusion pathway is in accordance with their theoretical proposal.

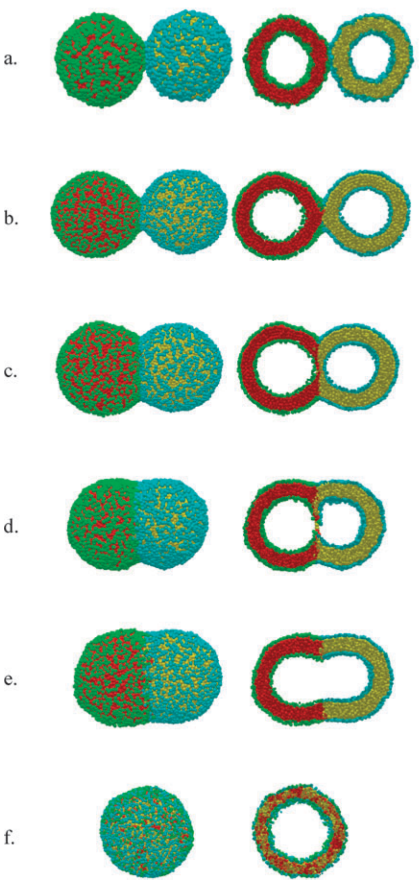

Fig. 3 Sequential snapshots of the fusion pathway FUS-I of two-component polymeric vesicles in the simulation at t = (a) 56.0 ns, (b) 238.0 ns, (c) 378.0 ns, (d) 665.0 ns, (e) 700.0 ns, and (f) 3500.0 ns.

When the value $a_{\mathrm{B}\alpha\mathrm{B}\beta}$ is increased to a larger one, an alternate fusion pathway (FUS-II) is observed, as shown in Fig. 4. In this fusion pathway, it starts still two vesicles contact and forms an early stalk (Fig. 4a) to a later trans-monolayer contact state (Fig. 4b); however, the trans-monolayer contact results in direct pore formation (Fig. 4c), rather than expansion of the contact area. Once the fusion pore is formed, it rapidly widens to yield complete fusion (Fig. 4d). This fusion pathway of vesicles is similar to what has been observed in low temperature by Noguchi and Takasu[8]and it agrees well with the prediction by the modified stalk model.[6]

As described by Grafmüller *et al.*,[15] the fusion time depends strongly on the initial tension of vesicle. To obtain the surface tension values, the amphiphilic bilayer, which has been used to compute the diffusion constant, is simulated in a periodic box. And the surface tension is determined by integrating the

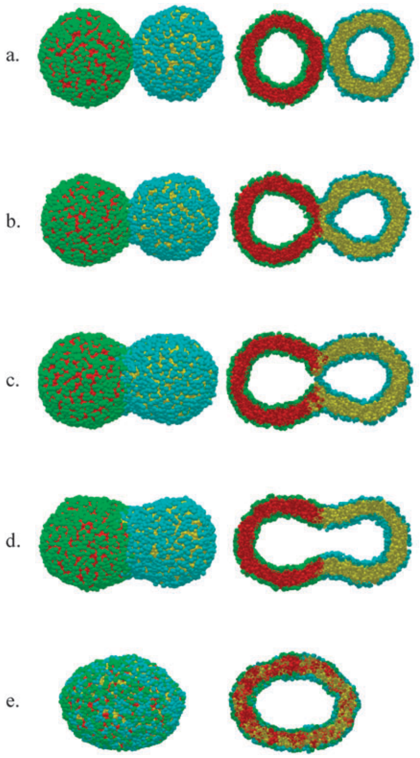

Fig. 4 Sequential snapshots of the fusion pathway FUS-II of two-component polymeric vesicles in the simulation at t = (a) 56.0 ns, (b) 241.5 ns, (c) 266.0 ns, (d) 280.0 ns, and (e) 3500.0 ns.

difference between normal and tangential stress across the interface separating the two segregated components *via* the formula:

$$\begin{aligned}\Sigma_{\mathrm{DPD}} &= \int [P_{xx}(x) - 0.5 \times (P_{yy}(x) + P_{zz}(x))]\,\mathrm{d}x \\ &= \frac{1}{A}\sum_{i<j}(F_{ij,x}x_{ij} - 0.5 \times (F_{ij,y}y_{ij} + F_{ij,z}z_{ij})).\end{aligned} \tag{10}$$

The simulated surface tension of the bilayer can be plotted as a function of the area per amphiphilic molecule, as shown in Fig. 5. From this Figure, we find the bilayer is tensionless for $A_0 \simeq 1.15r_\mathrm{c}$, and the area expansion modulus, K_a, of the bilayer close to the zero tension state is obtained directly from the slope of the curve giving a value of 12.78. Then the surface tension has a simple form in small tension regime,

$$\Sigma_{\mathrm{DPD}} = 12.78 \times (A - A_0)/A_0 = 11.11 \times (A - 1.15). \tag{11}$$

For vesicle fusion pathway FUS-I, an average surface tension of approximation 0.46 is obtained for the initial vesicle. And the simulated value of surface tension for FUS-II is estimated to be 4.74. Compared these two different vesicle fusion pathways, we find that for relatively large tension, the two-component polymeric vesicles proceed in a rapid manner to complete fusion in this fusion process, whereas for small tension, the amphiphilic molecules exchange between the bilayers is slowed down leading to an extended disk-like bilayer consisting of both inner monolayers and long fusion times. These observations are accordance with the investigation and analysis by Grafmüller *et al.*[15]

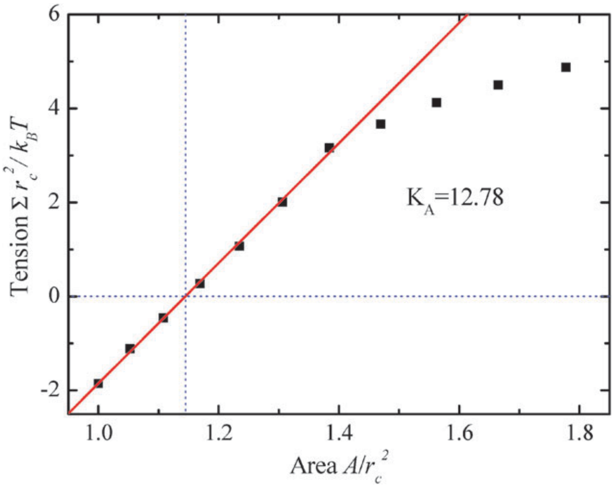

Fig. 5 Functional dependence of the surface tension on the area per amphiphile for A1B8A1 triblock copolymer system.

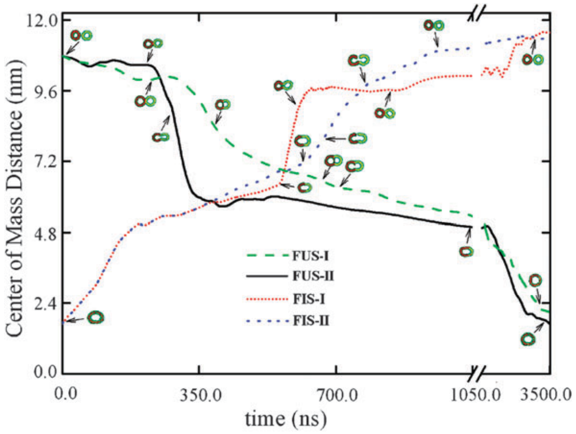

Fig. 6 Typical distance between the centers of mass of the vesicles in the simulations for different parameters shown in Table 1.

A more direct means of tracking fusion processes of two-component polymeric vesicles is given by observing the distance between the centers of the two vesicles with the time development, which can be seen from Fig. 6. In this Figure, the symbols FUS-I and FUS-II represent the fusion pathways in the original and modified stalk model, respectively. We find the hemifused intermediate in the FUS-I can remain within a period of approximately 420.0 ns before the fusion pore appears. Moreover, the distance decreases slowly after a stalk is formed; however, the distance decreases rapidly in FUS-II after the formation of the stalk, which indicates that the two-component polymeric vesicles proceed in a rapid manner to complete fusion. Subsequently, the particles belong to different types of amphiphilic molecules diffuse to each other and the distance decreases further. Finally, a larger vesicle with an approximately homogeneous distribution is obtained.

3.2 Vesicle fission

The initial configuration for the fission dynamics of the two-component polymeric vesicle is derived from the final configuration of vesicle fusion. As suggested by Laradji and

Kumar in ref. 29, large repulsive interaction parameters between two different types of amphiphilic molecules are needed to obtain fission. Hence, the repulsive parameters $a_{A\alpha A\beta}$ and $a_{B\alpha B\beta}$ are considered to be increased. Moreover, in order to prevent small micelles separate from the parent vesicle before sufficient domain growth, these repulsive parameters are required to be increased slowly. In view of these, a strategy is developed by means of a functional dependence of the repulsive parameters on rate r that increases gradually from 0 at the initial state to 1 after 350.0 ns. Specifically, in our simulations,

$$a_{A\alpha A\beta} = a_{B\alpha B\beta} = a_{ij,\min} \times (1.0 - (1.0 - e^{-2r})) + a_{ij,\max} \times (1.0 - e^{-2r}), \tag{12}$$

where $a_{ij,\min} = 25$ and $a_{ij,\max} = 100$ are, respectively, the minimum and maximal repulsive parameters. After 350.0 ns, a vesicle with two large domains is obtained, as shown in Fig. 7b. After that, an additional 3150.0 ns is simulated, the shape of vesicle changes to prolate. However, the prolate vesicle remains stable and complete fission is not obtained. As described in previous simulations based on DPD model,[28,29,42] the large repulsive interaction parameters are selected so that the vesicle is impermeable to solvent particles, which implies that the number of solvent particles in the interior of vesicle is constant. Thus, it is hard to complete fission without changing the interior volume of the vesicle. According to previous theoretical predicions,[21–24] complete fission can be obtained by reducing the reduced volume or introducing an asymmetry in the composition between two halves of the membrane. In our simulations, a reduction of the reduced volume can be obtained by either reducing the number of interior solvent particles of vesicle or increasing the system temperature. An asymmetry membrane can be induced by changing the architectures of the two types of amphiphilic molecules.

After a vesicle with two larger domains is formed, 30% of the solvent particles are removed from its interior and placed into the outer region, and complete fission is obtained, as shown in Fig. 7. First, deformation of the parent vesicle results in a shape change from prolate into a dumbbell, that is, two spheres connected by a narrow neck (Fig. 7c). Contraction of the neck results in these two spheres being connected by a very narrow neck and, thus, the opposing two monolayers attract and contact each other at the region of the very narrow neck (Fig. 7d) and the interior solvents are split into two parts. A breakdown of the inner monolayers then occurs at the region of the very narrow neck and a hemifission intermediate, in which the inner monolayers is separated into two parts while the outer monolayers is still in contact, is obtained (Fig. 7e). Finally the two spherical vesicles are separated from each other and the vesicle fission is complete (Fig. 7f). This fission process of vesicles is like a mirror image of the stalk model for the fusion pathway FUS-II of such vesicles. Fig. 7b–e correspond to the fused vesicle, fusion pore, trans-monolayer contact state and the stalk, which can be treated as the inverse processes of Fig. 4a–d, respectively.

An alternate fission pathway is obtained when we increase the temperature (K_BT) from 1.0 to 1.1, as shown in Fig. 8. In this fission process, it is also initiated by the formation of a vesicle with two larger domains (Fig. 8a). A cleavage of the membrane occurs at the region of the domain boundary (Fig. 8b), then the two opposing large domains repel each other results in a reduction of the contact area between these two domains, meanwhile, the two large domains reform their shapes spontaneously and two opposing bowl-shaped bilayer membranes are formed (Fig. 8c–e). Subsequently, the bowl-shaped membranes fluctuate and encapsulate solvent particles and form vesicles. Finally the merge of membranes occurs and the vesicle fission is complete (Fig. 8f).

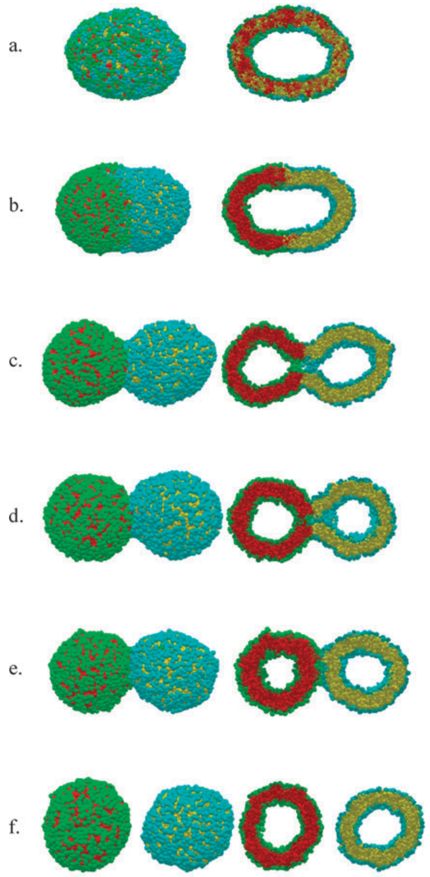

Fig. 7 Sequential snapshots of the fission pathway FIS-I of two-component polymeric vesicles in the simulation at t = (a) 0.0 ns, (b) 560.0 ns, (c) 602.0 ns, (d) 672.0 ns, (e) 840.0 ns, and (f) 1736.0 ns.

These two different fission pathways have been found by Yamamoto and Hyodo in a previous DPD simulation study.[26] However, a more clear observation to understand these fission processes can be found from our simulations due to the only two large domains in the original vesicle. In the fission pathway FIS-I, the shape transformations of the vesicle from prolate, to dumbbell (or pear), to two spheres connected by a very narrow neck, to complete fission are obtained, which can be compared well with experimental observation[43] and theoretical prediction based on area-difference model for budding transformation.[22]

In the fission pathway FIS-II, the reduction of the contact area between the two larger domains results in the formation of two opposing bowl-shaped bilayer membranes, and the two

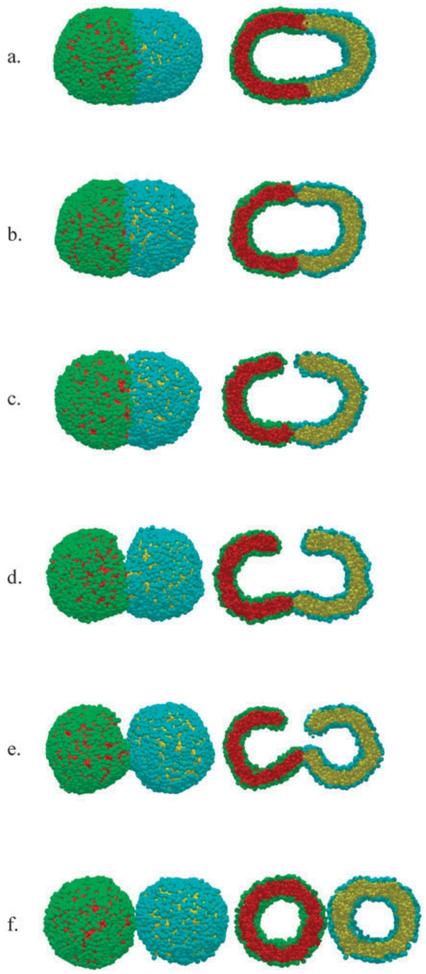

Fig. 8 Sequential snapshots of the fission pathway FIS-II of two-component polymeric vesicles in the simulation at t = (a) 350.0 ns, (b) 616.0 ns, (c) 672.0 ns, (d) 728.0 ns, (e) 840.0 ns, and (f) 952.0 ns.

daughter vesicles are formed from the bowl-shaped membranes almost at the same time, which is different from their observation that the parent vesicle reformed the cleavage and expelled the microvesicle. Moreover, the initial configuration for these fission processes of vesicle is derived directly from the final configuration of vesicles fusion. It is reasonable to compare the fusion and fission pathways from our simulations. We find that the fission pathway FIS-I of vesicles is like a mirror image of the stalk model for the fusion pathway FUS-II of such vesicles. Furthermore, since the amphiphilic triblock copolymers are modeled in our simulations, it gives us a choice to explore the fission dynamics of single-component vesicles with asymmetric membranes. To our knowledge, it is the first time to study the fission dynamics of single-component vesicles with asymmetric membranes using particle-based models.

For the fission process of single-component vesicles, it is well known that this process can be induced by a spontaneous curvature of the membrane.[21,22] For single-component vesicles consisting of amphiphilic ABC triblock copolymers, the spontaneous curvature of the membrane can be controlled by changing the repulsive interaction parameters between two different hydrophilic particles. A difference in repulsive interactions between two different hydrophilic particles introduces an asymmetric membrane, resulting in a spontaneous curvature. In case the membrane forms a vesicle, the spontaneous curvature of the membrane will influence the vesicle shapes, resulting in a complete fission. In our simulations, the amphiphilic membrane is essentially a single monolayer with the amphiphilic molecule responsible for the hydrophobic core as well as both hydrophilic ends. The spontaneous curvature of the single monolayer is controlled by the difference in repulsive parameters, Δa, between the hydrophilic blocks of the amphiphilic molecules. The sequential snapshots of this fission pathway are shown in Fig. 9. First, the vesicle shape is spherical (Fig. 9a). As Δa is increased, the prolate shape is formed from the spherical vesicle (Fig. 9b). Further increase in Δa causes formation of branches resulting in dumbbell and pear-shaped vesicles (Fig. 9c–e). These finally transform to fission-produced vesicles through a neck-like early intermediate and a hemifission late intermediate (Fig. 9f). Interestingly, two spherical vesicles have the same composition as the parent vesicle. We obtain this fission pathway in 21 among 30 fission events. In other fission events, the pear-shaped (or dumbbell) vesicle remains stable, the neck elongates continuously, rather than it ruptures. This fission pathway is in agreement with theoretical predictions.[21,22] The spontaneous curvature can also be controlled by varying the

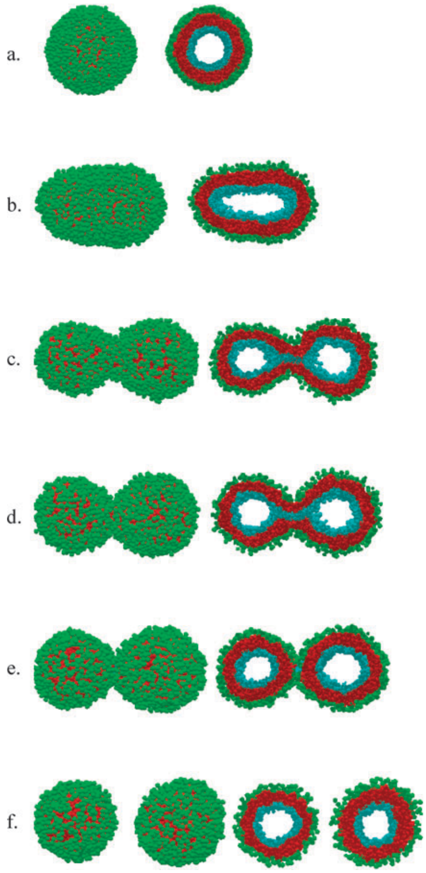

Fig. 9 Sequential snapshots of the fission pathway FIS-I of single-component vesicles with polymer-based asymmetric membranes in the simulation at t = (a) 0.0 ns, (b) 28.0 ns, (c) 126.0 ns, (d) 252.0 ns, (e) 420.0 ns, and (f) 1260.0 ns.

systemic temperature. The result of such simulation shows that increasing the temperature, indeed, results to complete fission. Since there is no domain boundary in the parent vesicle, only the fission pathway FIS-I is observed, which is different to the distinct fission pathway of two-component polymeric vesicles.

3.3 Compared vesicles fusion and fission pathways

As both fusion and fission have been observed, the fusion and fission pathways of polymeric vesicles can be compared. A schematic illustration of the different fusion and fission pathways of polymeric vesicles are also shown in Fig. 6. Although vesicle fusion and fission are each other's inverse processes, their pathways are not simply each others reverse, that is, vesicle fusion proceeds *via* stalk expansion, which can either rapidly form a fusion pore or remain in a hemifusion diaphragm. On the other hand, vesicle fission proceeds *via* a narrow neck or a cleavage along the domain boundary. However, both pathways also have some similarities. For example, the fission process FIS-I of two-component polymeric vesicles can be treated as a mirror image of the stalk model for the fusion process FUS-II of such vesicles. Therefore, it is possible to design different vesicle recycling pathways by varying the parameters described in our simulations. For example, for two-component vesicles, a parent vesicle can split into two smaller ones when the repulsive parameters of $a_{A\alpha A\beta}$ and $a_{B\alpha B\beta}$ are increased to larger ones. These two smaller vesicles can contact each other again and fuse into a larger one when these parameters are decreased. For single-component vesicles with polymer-based asymmetric membranes, an increase of the systemic temperature can result in complete fission, while the daughter vesicles can fuse into a larger one with the increase of temperature. A similar recycling pathway can be obtained by changing the hydrophilic parameters. These processes can be relevant to those physical processes of a real system that are caused by changing the systemic temperature or the selectivity of the solvents.

4. Conclusion

In this paper, we studied the fusion and fission pathways of polymeric vesicles by particle-based models of amphiphilic triblock copolymers using the dissipative particle dynamics (DPD). The amphiphilic molecule is built from two hydrophilic blocks and a hydrophobic middle block. We have shown that even using relatively simple models for amphiphilic triblock copolymers, many characteristics of amphiphiles in a dilute solution can be elucidated, such as their self-assembly into bilayer membranes and spontaneous formation of vesicles, as well as the distinct fusion and fission pathways of such vesicles. The appearance of two completely different fusion and fission pathways of two-component polymeric vesicles suggest that the computational modeling is robust against the details of the methods and they may be helpful in explaining the fusion and fission dynamics of membrane vesicles. Moreover, the fission dynamics of single-component vesicles with polymer-based asymmetric membranes has also been studied in the simulations. Interestingly, the daughter vesicles have the same composition as the parent vesicle and only one fission pathway has been observed. In addition, the fusion and fission pathways have been compared and distinct vesicle recycling pathways have been suggested from the simulations. It is confirmed that DPD simulation is an effective simulation technique for investigating and understanding the general principles of vesicle dynamics.

Acknowledgements

We are grateful for the financial support provided by the Outstanding Youth Fund (No. 20525416) and the Program of the National Natural Science Foundation of China (Nos. 20874094 and 50773072), NBRPC (No. 2005CB623800) and SRFDP (No. 20050358018). Parts of the simulations were carried out at the Shanghai Supercomputer Center (SSC).

References

1 L. V. Chernomordik and M. M. Kozlov, *Annu. Rev. Biochem.*, 2003, **72**, 175.
2 J. S. Bonifacino and B. S. Glick, *Cell*, 2004, **116**, 153.
3 V. S. Markin, M. M. Kozlov and V. L. Borovjagin, *Gen. Physiol. Biophys.*, 1984, **3**, 361.
4 L. V. Chernomordik, M. M. Kozlov and J. Zimmerberg, *J. Membr. Biol.*, 1995, **146**, 1.
5 L. V. Chernomordik, G. B. Melikyan and Y. A. Chizmadzhev, *Biochim. Biophys. Acta*, 1987, **906**, 309.
6 D. P. Siegel, *Biophys. J.*, 1993, **65**, 2124.
7 G. J. A. Sevink and A. V. Zvelindovsky, *Macromolecules*, 2005, **38**, 7502.
8 H. Noguchi and M. Takasu, *J. Chem. Phys.*, 2001, **115**, 9547.
9 M. Müller, K. Katsov and M. Schick, *Biophys. J.*, 2003, **85**, 1611.
10 S. J. Marrink and A. Mark, *J. Am. Chem. Soc.*, 2003, **125**, 11144.
11 M. J. Stevens, J. H. Hoh and T. B. Woolf, *Phys. Rev. Lett.*, 2003, **91**, 188102.
12 J. C. Shillcock and R. Lipowsky, *Nat. Mater.*, 2005, **4**, 225.
13 P. M. Kasson, N. W. Kelley, N. Singhal, M. Vrljic, A. T. Brunger and V. S. Pande, *Proc. Natl. Acad. Sci. U. S. A.*, 2006, **103**, 11916.
14 V. Knecht, A. E. Mark and S. J. Marrink, *J. Am. Chem. Soc.*, 2006, **128**, 2030.
15 A. Grafmuller, J. C. Shillcock and R. Lipowsky, *Phys. Rev. Lett.*, 2007, **98**, 218101.
16 L. H. Gao, R. Lipowsky and J. C. Shillcock, *Soft Matter*, 2008, **4**, 1208.
17 D. E. Discher and A. Eisenberg, *Science*, 2002, **297**, 967.
18 Y. B. Xu, F. Zhang, Z. L. Su, J. A. McNew and Y. K. Shin, *Nat. Struct. Mol. Biol.*, 2005, **12**, 417.
19 Y. F. Zhou and D. Y. Yan, *J. Am. Chem. Soc.*, 2005, **127**, 10468.
20 W. Su, Y. H. Luo, Q. Yan, S. Wu, K. Han, Q. J. Zhang, Y. Q. Gu and Y. M. Li, *Macromol. Rapid Commun.*, 2007, **28**, 1251.
21 U. Seifert, K. Berndl and R. Lipowsky, *Phys. Rev. A*, 1991, **44**, 1182.
22 L. Miao, U. Seifert, M. Wortis and H. G. Dobereiner, *Phys. Rev. E*, 1994, **49**, 5389.
23 U. Seifert, *Phys. Rev. Lett.*, 1993, **70**, 1335.
24 C. M. Chen, P. G. Higgs and F. C. MacKintosh, *Phys. Rev. Lett.*, 1997, **79**, 1579.
25 I. R. Cooke, K. Kremer and M. Deserno, *Phys. Rev. E*, 2005, **72**, 011506.
26 S. Yamamoto and S. Hyodo, *J. Chem. Phys.*, 2003, **118**, 7937.
27 H. Noguchi, *Phys. Rev. E*, 2003, **67**, 041901.
28 M. Laradji and P. B. S. Kumar, *Phys. Rev. Lett.*, 2004, **93**, 198105.
29 M. Laradji and P. B. S. Kumar, *J. Chem. Phys.*, 2005, **123**, 224902.
30 E. Atilgan and S. X. Sun, *J.Chem. Phys.*, 2007, **126**, 095102.
31 A. J. Markvoort, A. F. Smeijers, K. Pieterse, R. A. van Santen and P. A. J. Hilbers, *J. Phys. Chem. B*, 2007, **111**, 5719.
32 B. B. Hong, F. Qiu, H. D. Zhang and Y. L. Yang, *J. Phys. Chem. B*, 2007, **111**, 5837.
33 B. M. Discher, Y. Y. Won, D. S. Ege, J. C. M. Lee, F. S. Bates, D. E. Discher and D. A. Hammer, *Science*, 1999, **284**, 1143.

34 P. Alexandridis and B. Lindman, *Amphiphilic Block Copolymers: Self-Assembly and Applications*, Elsevier, New York, 2000.
35 Y. F. Zhou and D. Y. Yan, *Angew. Chem., Int. Ed.*, 2005, **44**, 3223.
36 P. J. Hoogerbrugge and J. M. V. A. Koelman, *Europhys. Lett.*, 1992, **19**, 155.
37 R. D. Groot and P. B. Warren, *J. Chem. Phys.*, 1997, **107**, 4423.
38 R. D. Groot and T. J. Madden, *J. Chem. Phys.*, 1998, **108**, 8713.
39 M. Serrano, G. De Fabritiis, P. Espanol and P. V. Coveney, *Math. Comput. Simul.*, 2006, **72**, 190.
40 R. Goetz and R. Lipowsky, *J. Chem. Phys.*, 1998, **108**, 7397.
41 L. H. Gao, J. Shillcock and R. Lipowsky, *J. Chem. Phys.*, 2007, **126**, 015101.
42 A. J. Markvoort, R. A. van Santen and P. A. J. Hilbers, *J. Phys. Chem. B*, 2006, **110**, 22780.
43 Y. Inaoka and M. Yamazaki, *Langmuir*, 2007, **23**, 720.